공학석사 학위논문

On the Study of a Robust History Matching of Facies Model by Distance-based Method and Ensemble Kalman Filter

거리기반방법과 앙상블칼만필터를 이용한

암종모델 히스토리매칭 연구

2016 년 2 월

서울대학교 대학원

에너지시스템공학부

임 서 진

Abstract

On the Study of a Robust History Matching of Facies Model by Distance-based Method and Ensemble Kalman Filter

Seojin Lim

Department of Energy Systems Engineering

The Graduate School

Seoul National University

This paper develops a robust history matching method that improves prediction performance of facies models and evaluates interwell connectivity by integrating dynamic and static data. Previous studies have been focused on matching history based on dynamic data. Thus, it is impossible to predict static properties and facies distribution and this results in deterioration of reliability of production estimation. The developed method predicts facies distribution by selecting training images among multiple training images using distance-based method. Reservoir models are regenerated from the selected training images

and history matched. The method predicts interwell connectivity accurately with 88.7% probability. The prediction performance is improved by 70.9% lower error than the conventional method. The proposed method reliably predicts the fluid production behavior of reservoir without breakthrough information. This paper can improve the prediction performance of fluid production. This can contribute to a reasonable production design based on reliable facies models obtained from the integration of dynamic and static data.

Table of Contents

List of Tables

List of Figures

viii

1. Introduction

History matching is an inverse modeling to generate geomodels that shows similar production behavior with observed production history. It is necessary to predict and optimize future production performance but challenging since it is impossible to get a solution that is identical to the earth due to the ill-posed nature of the history matching. Thus, reliable optimization method is needed for reliable prediction of production performance in history matching.

History matching algorithms can be categorized as the gradient based method and the non-gradient based method. Anterion et al. (1989) suggested analytical method using continuous equation and newton method and applied to history matching. The results were accurate in case a proper extrapolation method was used. Roggero et al. (1998) integrated gradual deformation method (GDM) to the gradient based method for preservation of geostatistical information. However, the gradient based methods have risk that converge to local minimum. To overcome the local minimum problem, the non-gradient based method was suggested. Soleng (1999) showed applicability of genetic algorithm (GA) for history matching by finding optimum solution in history matching of PUNQ-S3 reservoir. Schluze-Riegert et al. (2002) applied evolutionary algorithm (EA) and successfully matched history of bottom hole pressure (BHP) and fluid production performance. The non-gradient based methods have limitation that it is hard to mimic geologic trends since it perturbs reservoir properties in a random manner. The previous history matching methods are not able to preserve static data since it focuses on matching dynamic data and ignored static information.

Nowadays, Ensemble Kalman Filter (EnKF), the method that can characterize properties of reservoirs, is widely used in history matching. This method was first introduced to history matching by Nævdal and Vefring (2002) who reproduce the permeability distribution of synthetic reservoirs using EnKF. Gu and Oliver (2005) reproduced both permeability and porosity distribution using EnKF.

However, history matching with facies description is still challenging. Sarma and Chen (2009) and Lorentzen et al. (2012) integrated kernel method and level set method into EnKF for history matching of facies models respectively. They improved history matching performance but there were limitation in prediction of fluid production due to failure in prediction of facies distribution.

The objective of this study is developing a robust history matching method that improves prediction performance of facies model and is able to evaluate interwell connectivity by integrating dynamic and static data. The method relies on preprocess of facies model using distance-based method before history matching with EnKF. The method predicts facies distribution by selecting training images among multiple training images stochastically generated from static information using distance-based method. The distance-based method allows selecting geomodels that show similar production behavior with true history data by defining distance based on dynamic data. Reservoir models are regenerated from the selected training images. Part of reservoir models are selected from clustering to improve accuracy of prediction of facies distribution and history matched. The flow of the developed method is shown in **Figure 1.1**.

This research consists of 5 chapters. Chapter 1 is introduction. Limitations of previous researches are revealed and the objective of this research is presented. Chapter 2 is theoretical background. Multiple-point geostatistics, distance-based method and Ensemble Kalman Filter that are used for characterization of facies models and history matching are explained. In chapter 3, the new robust history matching method is proposed. In chapter 4, the proposed method is validated. Conclusions are presented in chapter 5.

Figure 1.1 Procedure for characterization of channel reservoir and performance prediction.

2. Theoretical background

2.1. Multiple-point Geostatistics

The veriogram based method has been generally used for generating reservoir models. However, it has limitation that is hard to represent geological patterns since it uses only two-point information. Therefore, multiple-point geostatistics is used for facies modeling. Unlike two-point geostatistics, multiple-point geostatistics can generate reservoir models having geological patterns since it captures patterns from a training image by considering spatial information of multiple points.

2.1.1. Training image

A training image is a description of a geologic pattern. **Figure 2.1** is the schematic diagram of model generation from training image. Training image doesn't have geologic information of specific location. The pattern of the training image is reproduced in reservoir models constraining facies of specific spots known from core data.

The size of training image is important. Training image should be large more than twice reservoir models to be generated to reproduce channels without breaks. On the other hand, smaller training image than reservoir models should be used to reproduce small scale pattern.
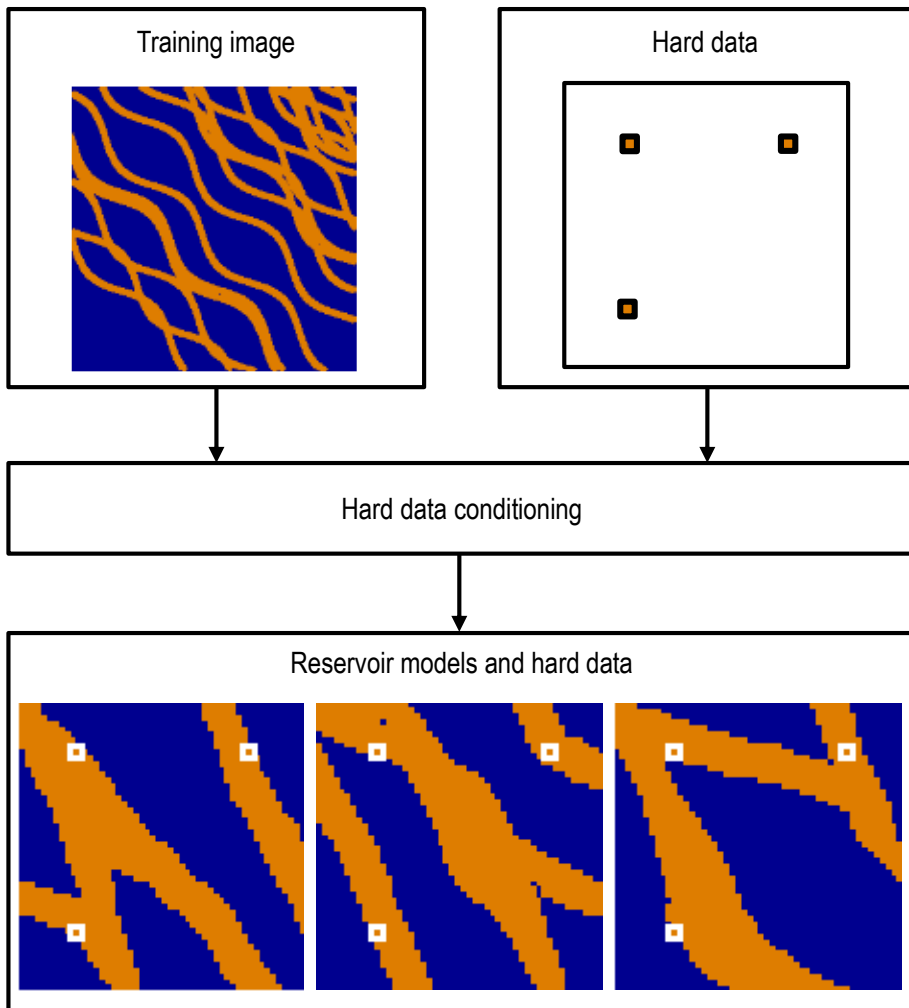
Figure 2.1 Procedure of reservoir model generation using multiple-point geostatistics.

2.1.2. Single normal equation simulation (Snesim)

After generation of training image, a method to reproduce patterns of training image in reservoir models while core data is preserved is required. One of multiple-point geostatistics, Snesim (Guardiano and Srivasta, 1993) calibrates probability of each facies at every point from training image by considering multiple points nearby. For example, corresponding pattern to '?' exists at three points in the training image of the **Figure 2.2**. The facies of '?' is 'Cat 1' at one point and 'Cat 0' at two points. Therefore, the probability to be 'Cat 1' at '?' is 1/3. Strebelle (2002) applied search tree to make the simulation efficient. Search tree saves conditional probability of every case by scanning training image only once.

The procedure of Snesim is as follows (Lee, 2014).

Step1. Data template is defined.

Step2. A training image is scanned by data template. Spatial distribution of the training image is saved as conditional probability in a search tree.

Step3. Static data is located in a grid system. Random path is defined.

Step4. A case which corresponds to the facies information of visited grid is searched in the search tree. Facies is allocated in the visited grid depending on conditional probability of the case.

Step5. Step4 is repeated following the random path until facies is allocated in every grid.

Reservoir models are generated from a training image by this simulation procedure.
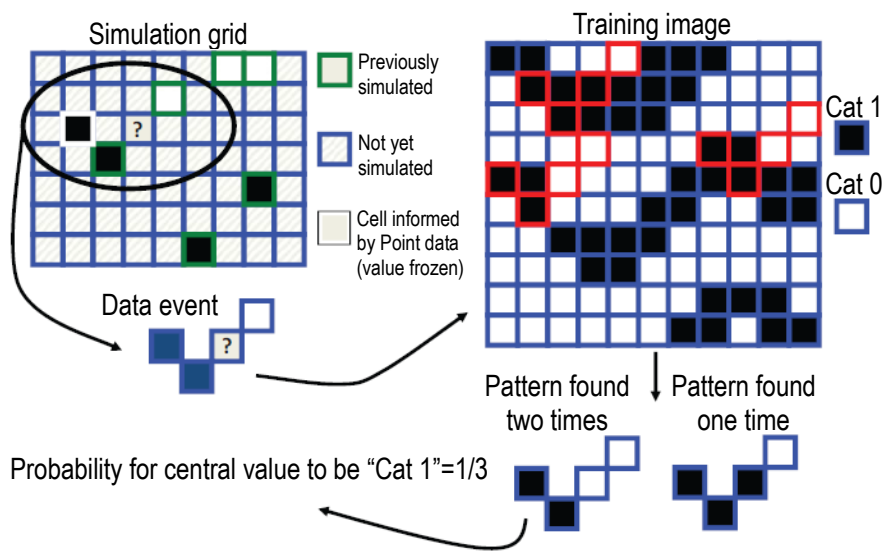
Figure 2.2 Scanning of a training image for probability evaluation (modified from Caers, 2011).

2.2. Distance-based method

2.2.1. Concept of distance-based method

Distance quantifies dissimilarity between two models. The closer the distance is, the similar the reservoir models are. Distance can be defined by anything but should be highly correlated with the interested object.

Distance is classified into dynamic based distance and static based distance. Static based distance is the distance defining dissimilarity based on appearance such as facies distribution and connected hydrocarbon volume (CHV). Dynamic based distance is the distance defined by dynamic data which are interested or highly related to the interested object. For example, well oil production rate (WOPR) and well water cut (WWCT). Suzuki and Caers (2006) showed static based distance can be used for history matching by integrating Hausdorff distance to searching algorithm. Scheidt and Caers (2009) showed dynamic based distance can be used for uncertainty analysis.

The dynamic based distance have advantage that the distance from true value is known but is time consuming since it needs forward simulation. In this research, dynamic based distance is used to determine geologic patterns of reservoirs.

The general form of distance calculation between model x_a and x_b is Minkowski model as shown in equation (2.1) (Park, 2008).

$$d(x_a, x_b) = \left[\sum_{i=1}^{T} |(x_a)_i - (x_b)_i|^p \right]^{1/p} \tag{2.1}$$

Where, $(x)_i$ is i^{th} element of vector x. T is the number of total observation time. p is the variable defining the distance space. p equals 2 if the space is Euclidian space. If distances between N reservoir models are calculated, N × N distance matrix is made and can be visualized in 2 dimensional space by multi-dimensional scaling (MDS).

2.2.2. k-medoid clustering

Clustering is a grouping method that can group models having similar characteristics. Clustering allows selecting models showing similar production behavior without analyzing production behaviors one by one. The procedure of k-medoid clustering used in this research is as follows. It is illustrated in **Figure 2.3**. Cluster centers are selected among existing points in a distance space.

Step1. Cluster centers are selected randomly.

Step2. A distance from each cluster center to each model is calculated.

Step3. Each model is allocated in the cluster of the nearest cluster center.

Step4. The models of which the mean of distance is smallest among models in same cluster become new cluster centers.

Step5. Step 2-4 are repeated until the cluster centers don't change anymore.

(a) Step1   (d) Step5

(b) Step2-3   (c) Step4
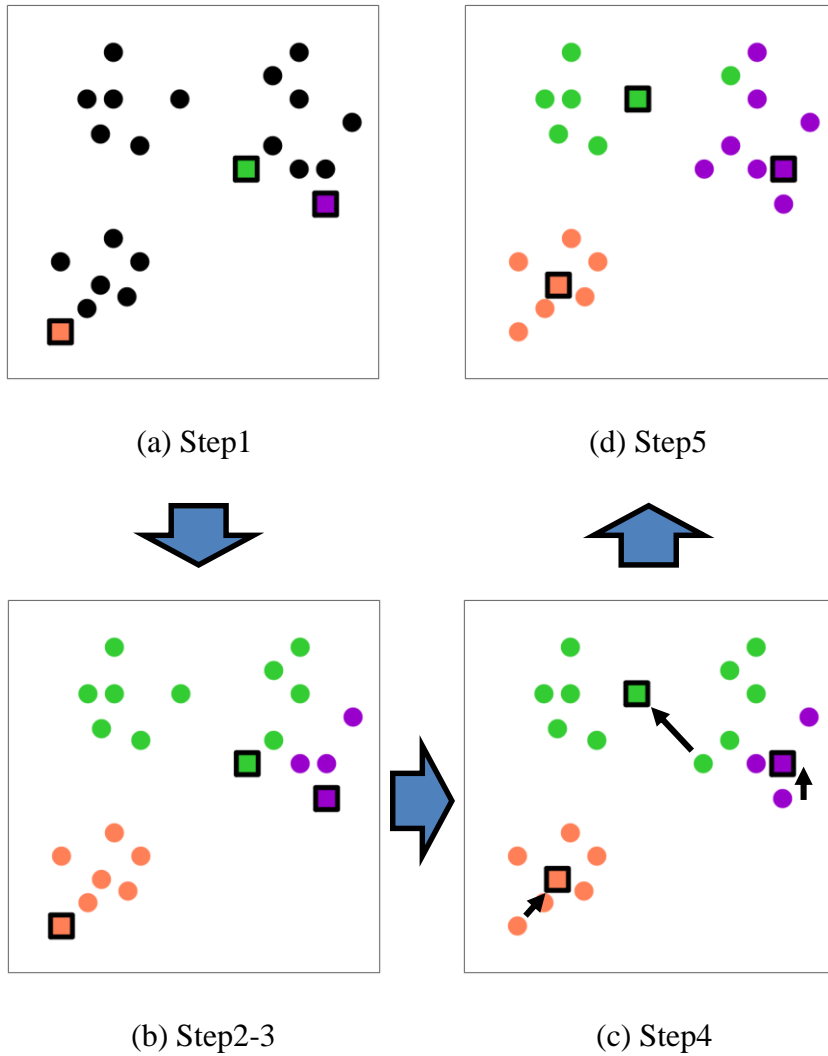
Figure 2.3 Procedure of k-medoid clustering: (a) Cluster centers chosen randomly, (b) allocation of models to each cluster, (c) cluster centers updated and (d) iteration of (b)-(c) until cluster centers are fixed.

2.2. Ensemble Kalman Filter

Ensemble Kalman Filter (EnKF) is composed of prediction step and assimilation step. In the prediction step, reservoir models are simulated from a present observation time to a next observation time. In the assimilation step, reservoir models are corrected based on observed data. The correction procedure is conducted using state vector x_k in equation (2.2) (Evensen, 1994). The state vector consists of three vectors: static variables, m_k^s, such as permeability and porosity, dynamic variables, m_k^d, such as pressure and saturation and model predictions, d_k, such as well oil production rate (WOPR) and well water cut (WWCT). A ensemble is a reservoir model.

$$
x_{k,j} = \begin{bmatrix} m_k^s \\ m_k^d \\ d_k \end{bmatrix}^j , \; j = 1, 2, \dots, N_e \tag{2.2}
$$

Where, k : observation time

j : j^{th} ensemble

The prediction step is conducted using initial ensembles. EnKF is time efficient method since it simulates all ensembles simultaneously. The equation (2.3) is input and output of the prediction step.

$$\begin{bmatrix} m_k^d \\ d_k \end{bmatrix} = f(m^s, m_{k-1}^d) \tag{2.3}$$

The assimilation step begins using observation data obtained from the prediction step. EnKF corrects ensembles to minimize estimated error covariance. The mean of state vectors from all ensembles is assumed to be the estimated error since the true state vector is unknown (equation (2.4)).

$$e_{k,j}^- \equiv x_k - \hat{x}_{k,j}^- \cong \bar{x}_k - \hat{x}_{k,j}^- \tag{2.4}$$

Where, $e_{k,j}^-$: estimated error

   x_k : true value of state vector

   $\hat{x}_{k,j}^-$: state vector of each ensemble

   $\bar{x}_k$: mean of state vectors from all ensembles

The estimated error covariance is calculated from the estimated error using equation (2.5).

$$P_k^- \equiv E\left[e_k^- e_k^{-T}\right] = \frac{1}{N_e - 1} \sum_{j=1}^{N_e} e_{k,j}^- e_{k,j}^{-T} \tag{2.5}$$

Where, P_k^- : estimated error covariance

N_e : the number of ensemble

j : j^{th} ensemble

Kalman gain, K_k is the weight vector that minimizes the estimated error covariance. It is calculated using equation (2.6). State vectors are updated using Kalman gain (equation (2.7)).

$$K_k = P_k^- H^T (H P_k^- H^T + R_k)^{-1} \tag{2.6}$$

$$\hat{x}_{k,j} = \hat{x}_{k,j}^- + K_k (d_{obs} + v_{k,j} - H_k \hat{x}_{k,j}^-) \tag{2.7}$$

Where, R_k : observation error covariance

H : observation vector

d_{obs}: observed data

$v_{k,j}$: observation error

$v_{k,j}$ is the error originated from measurement tool or method. It is random normalized error of which average is 0 and covariance is R_k. H is a vector composed of 0 and 1 in order to extract corresponding variables to observation data. Updated state vectors become input for the next prediction step.

3. Development of a new history matching method

This paper proposes a robust history matching method that integrates dynamic and static data using EnKF coupled with distance-based method. The proposed method considers static information by using multiple training images. By selecting proper training image, the method predicts spatial distribution of geologic facies accurately and improves performance of history matching. The procedure is described in **Figure 3.1**. The proposed method is consisted of three steps: the first step, selection of training image, is presented in section 3.1. The second step, reproduction of facies model, is presented in section 3.2. The last step, history matching with Ensemble Kalman Filter, is presented in section 3.3.
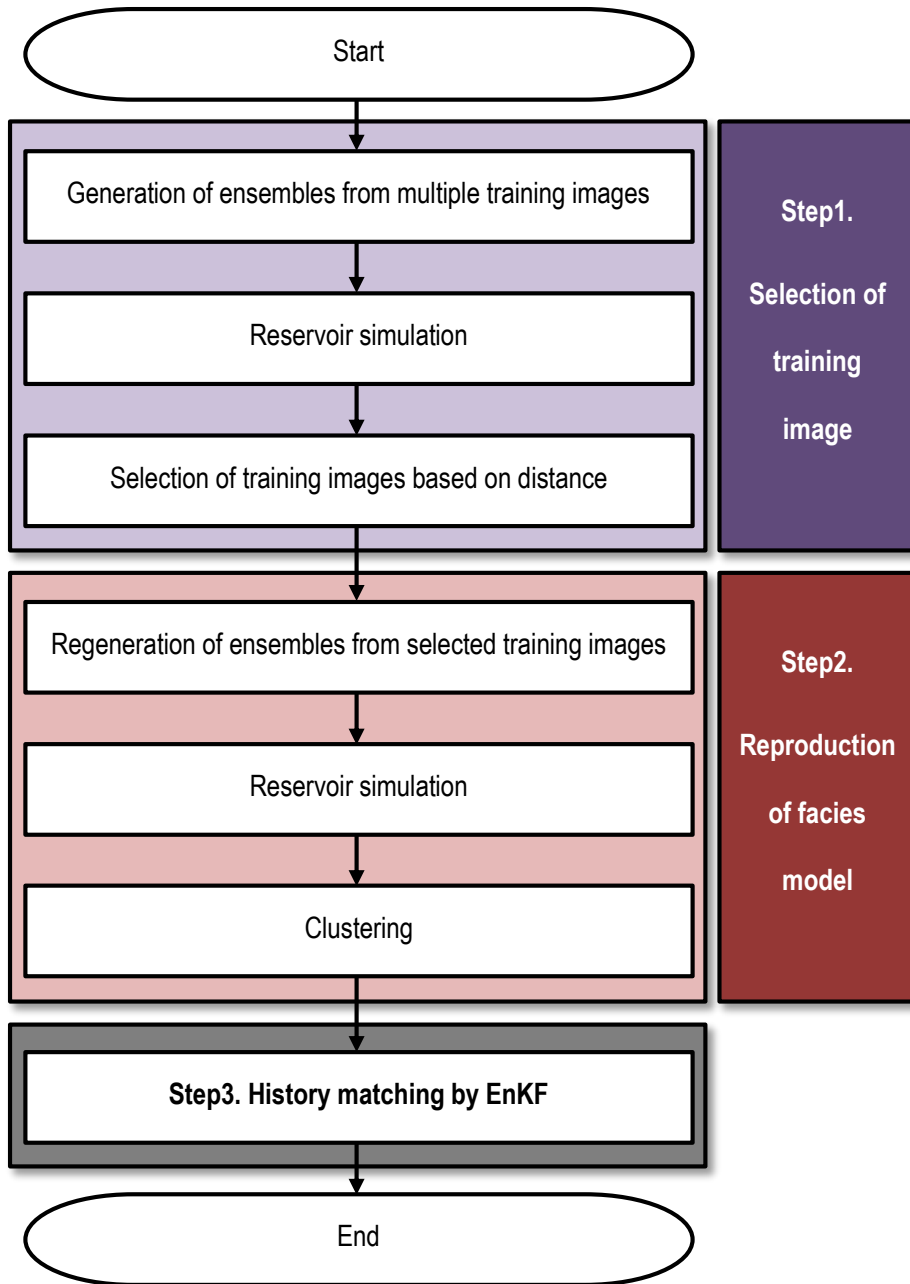
```
                          ┌──────────────────────────┐
                          │           Start          │
                          └──────────────────────────┘
                                       │
                                       ▼
    ┌────────────────────────────────────────────────────┐   ┌──────────────┐
    │  ┌──────────────────────────────────────────────┐  │   │              │
    │  │ Generation of ensembles from multiple training │ │   │   Step1.     │
    │  │                images                          │  │   │              │
    │  └──────────────────────────────────────────────┘  │   │ Selection of │
    │                      │                              │   │              │
    │                      ▼                              │   │   training   │
    │  ┌──────────────────────────────────────────────┐  │   │              │
    │  │            Reservoir simulation                │  │   │    image     │
    │  └──────────────────────────────────────────────┘  │   │              │
    │                      │                              │   │              │
    │                      ▼                              │   │              │
    │  ┌──────────────────────────────────────────────┐  │   │              │
    │  │ Selection of training images based on distance │  │   │              │
    │  └──────────────────────────────────────────────┘  │   │              │
    └────────────────────────────────────────────────────┘   └──────────────┘
                                       │
                                       ▼
    ┌────────────────────────────────────────────────────┐   ┌──────────────┐
    │  ┌──────────────────────────────────────────────┐  │   │              │
    │  │ Regeneration of ensembles from selected training│ │   │   Step2.     │
    │  │                images                          │  │   │              │
    │  └──────────────────────────────────────────────┘  │   │ Reproduction │
    │                      │                              │   │              │
    │                      ▼                              │   │  of facies   │
    │  ┌──────────────────────────────────────────────┐  │   │              │
    │  │            Reservoir simulation                │  │   │    model     │
    │  └──────────────────────────────────────────────┘  │   │              │
    │                      │                              │   │              │
    │                      ▼                              │   │              │
    │  ┌──────────────────────────────────────────────┐  │   │              │
    │  │                Clustering                      │  │   │              │
    │  └──────────────────────────────────────────────┘  │   │              │
    └────────────────────────────────────────────────────┘   └──────────────┘
                                       │
                                       ▼
    ┌────────────────────────────────────────────────────┐
    │  ┌──────────────────────────────────────────────┐  │
    │  │      Step3. History matching by EnKF           │  │
    │  └──────────────────────────────────────────────┘  │
    └────────────────────────────────────────────────────┘
                                       │
                                       ▼
                          ┌──────────────────────────┐
                          │            End           │
                          └──────────────────────────┘
```

**Figure 3.1. Flow chart of the proposed method.**

3.1. Selection of training image

In the selection step, facies distribution is predicted by selecting training image. Firstly, multiple training images are generated based on static data. Facies models are produced from training images. Secondly, the facies models are simulated. Lastly, distances between facies models are calibrated using dynamic data obtained from simulation to characterize facies distribution. The distance is defined as difference of production behavior between models. Distances between N+1 vectors which are N prediction vectors and 1 observed production history data vector are calculated by equation (3.1). As a result, facies models that show similar production behavior with the observed data are located nearby the reference field in a distance map. The closest 5 models from the observed history are selected in each distance map as shown in **Figure 3.2**. The reason why select 5 models is presented in Appendix A. Training images that generated the selected models become the source of reproduction.

$$d_{i,j} = \sqrt{(x_i - x_j)^T (x_i - x_j)}, \ i,j = 1, 2, \dots, \text{N}, \text{N} + 1 \tag{3.1}$$

Where, i, j : number of a reservoir model

  x : vector of production behavior
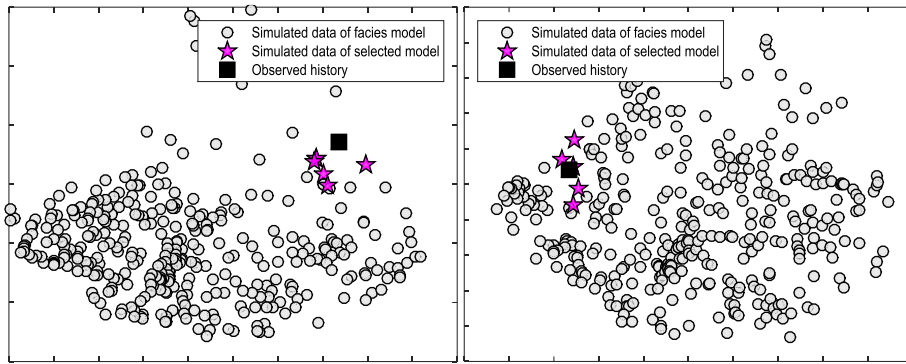
(a) WOPR of P1   (b) WOPR of P2

Figure 3.2 2D distance maps of response parameters: (a) WOPR of a production well P1 and (b) WOPR of the other production well P2.

3.2. Reproduction of facies model

In the reproduction step, ratio of facies models from each training image is adjusted. Among the training images selected in section 3.1., the closer the training image is to the observed production history, the more the training image reproduces facies models.

Regeneration ratio of facies model is determined depending on distance weight w_i^o defined as equation (3.2). Distance weight is proportion of a reciprocal of distances between the reservoir models selected and the observed history divided by the number of response parameters since the weight of each response parameter is all the same. Response parameter is object of history matching such as oil production rate and water cut. Each training image used to generate the ith reservoir model selected reproduces TI_i reservoir models as equation (3.3).

Reproduced facies models are simulated and distance is calculated from newly simulated data. Facies models allocated in same cluster with the observed production data are selected. **Figure 3.3** shows an example of facies model selection. In **Figure 3.3(a)**, observed production history is belong to cluster2. In **Figure 3.3(b)**, it is belong to cluster3. Facies models involved in cluster2 of **Figure 3.3(a)** and cluster3 of **Figure 3.3(b)** are selected. Sum of cluster2 of **Figure 3.3(a)** and cluster3 of **Figure 3.3(b)** becomes initial ensemble for history matching with Ensemble Kalman Filter. The number of cluster is determined as a number which makes the number of the sum around

100 since the minimum number of ensemble which allows Ensemble Kalman Filter operate without any serious error is it generally.

$$w_i^o = \frac{1}{N_o} \times \left(\frac{\frac{1}{d_i^o}}{\Sigma_{i=1}^5 \frac{1}{d_i^o}} \right) \tag{3.2}$$

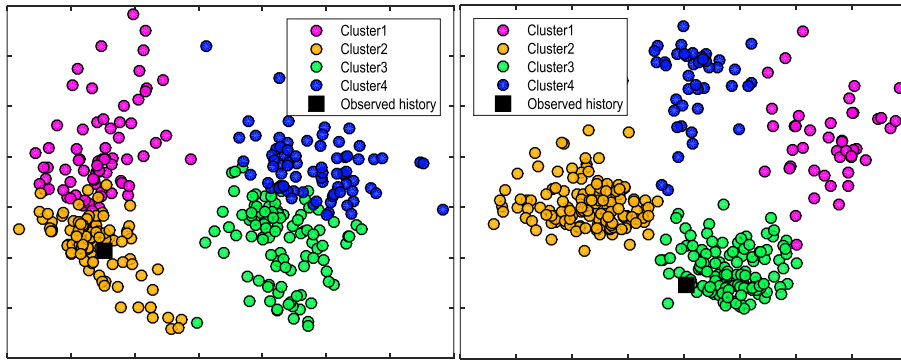$$TI_i = w_i^o \times N \tag{3.3}$$

Where, d_i^o : the distance between i^{th} reservoir model selected and the observed history

       o : number of the response parameter

       N_o : the number of the response parameters

       TI_i : the number of regenerated facies models using the training image from i^{th} reservoir model selected

       N : the number of initial reservoir models

(a) WOPR of P1   (b) WOPR of P2

Figure 3.3 Clustering and selection of facies models: (a) WOPR of a production well P1 and (b) WOPR of the other production well P2.

3.3. History matching with Ensemble Kalman Filter

History matching is performed using facies models obtained from the aforementioned preprocessing procedure. Ensemble Kalman Filter is used for the history matching. Permeability distribution is updated using production performance data newly simulated. Facies distribution data required for forward simulation is determined in the preprocessing step.

4. Results and discussion

A reservoir used for validation of the proposed model is a synthetic channeled reservoir. The assumptions used in characterization of facies model are as follows.

- Channeled reservoirs are consisted of two facies: sand and shale. The permeability and porosity of sand is 2,000 md and 0.3 respectively. That of shale is 20 md and 0.15.

- Flow behavior follows two phase flow: oil and water.

- History matching is conducted during 360 days and production behaviors are predicted until 1,800[th] day. Time step is 60 days.

- The number of initial ensemble is 360.

Channeled reservoir models are generated by SGeMS (Stanford Geostatistical Modeling Software) and history matched by EnKF. ECLIPSE100 of Schlumberger is used for forward simulation.

Average relative error is estimated for the quantitative evaluation of performance as equation (4.1).

$$Error = \frac{1}{N}\sum_{t=1}^{N}\frac{(Predicted\ Value - Observed\ value)}{Observed\ value} \times 100 \qquad (4.1)$$

Where, N : The number of observed time

The reference field is described in section 4.1. The result of preprocessing of facies model using the proposed method is presented in section 4.2. The performance prediction of the proposed method is evaluated in section 4.3. The effects of multiple training images are analyzed in section 4.4. The robustness of the method is verified in section 4.5. The discussion is in section 4.6.

4.1. Reservoir description

4.1.1 Reference field description

A reference field is cuboid reservoir of which the length and the width are 2,500 ft and depth is 20 ft. It has high permeable sand channel of 2,000 md and low permeable shale matrix of 20 md. The porosity of sand and shale are 0.3 and 0.15 respectively. The distribution of reference permeability and porosity are described in **Figure 4.1**. Relative permeability and capillary pressure curves of sand and shale are shown in **Figure 4.2** and **4.3** respectively. 400 STB of water is injected every day in one injector, I1. Oil is produced in two production wells, P1 and P2, under condition of 500 psia. The simulation information and well data are shown in **Table 4.1** and **4.2**.
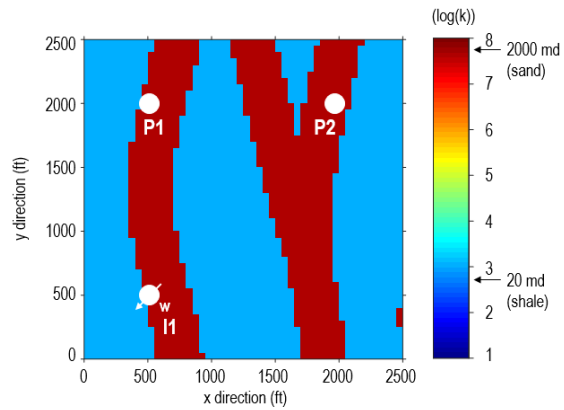
(a) Permeability (log md)
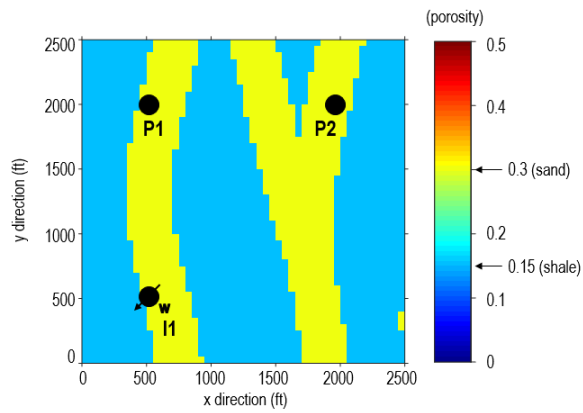
(b) Porosity (fraction)

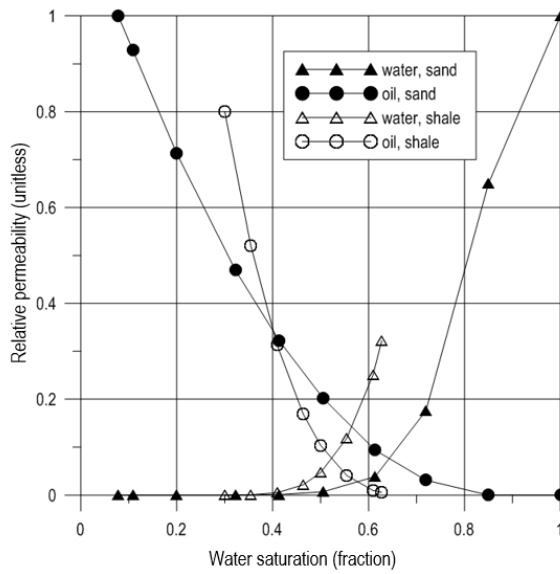**Figure 4.1 Permeability and porosity distribution of the reference field.**

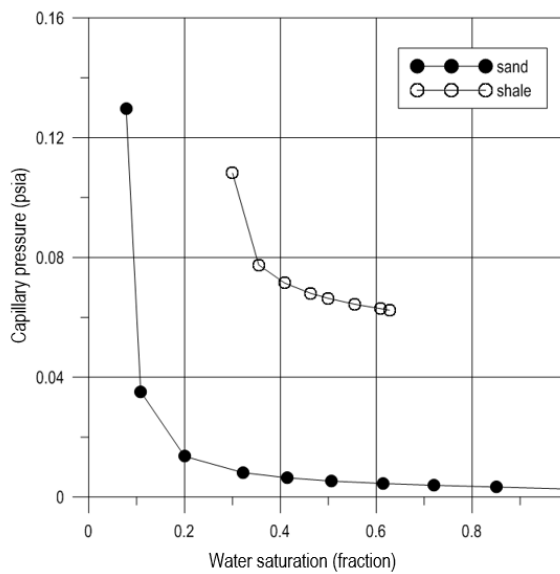**Figure 4.2 Relative permeability curves of sand and shale.**

Figure 4.3 Capillary pressure curves of sand and shale.

30

Table 4.1 Simulation information of the reference field and reservoir models

Property		Value
Grid size		50×50
Width (ft)		2,500
Length (ft)		2,500
Thickness (ft)		20
Porosity (fraction)	Sand	0.3
	Shale	0.15
Initial pressure (psia)		2,000
Permeability (md)	Sand	2,000
	Shale	20
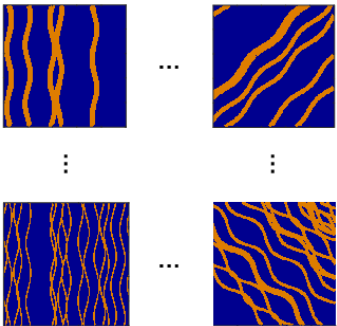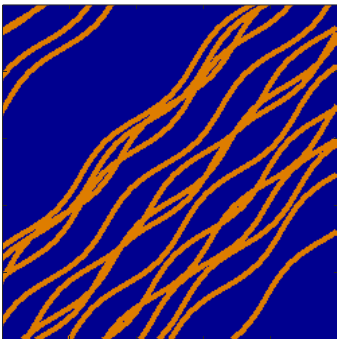
Table 4.2 Well information and boundary conditions of the reference field and reservoir models

| Well		Location (ft)	Control mode	Facies
Injection well	I1	(500, 500)	400 STB/day	Sand
Production well	P1	(500, 2,000)	500 psia	Sand
	P2	(2,000, 2,000)	500 psia	Sand

4.1.2. Comparison model description

The proposed model is compared with the conventional method which is the original Ensemble Kalman Filter without preprocessing of facies model. The difference between them is described in **Table 4.3**. The comparison model uses the training image of which the orientation is 45° and the width is 2 for generation of facies models. It matches history using Ensemble Kalman Filter.

Table 4.3 Comparison between the proposed model and the comparison model

Characteristic	The proposed model	The comparison model
Training image	Multiple training images 	Single training image Orientation: 45°, Width: 2
Methodology	Selection of training image ↓ Reproduction of facies model ↓ EnKF	EnKF

* Orientation:

4.2. Model development

Facies prediction is performed using the proposed method. Sensitivity analysis, selection of training image, reproduction of facies model and clustering are proceeded sequentially.

4.2.1. Sensitivity analysis

Distance-based generalized sensitivity analysis (DGSA, detailed explanation about DGSA is presented in Fenwick et al., 2014) is used for sensitivity analysis of uncertainty parameters in generation of training image. Uncertainty parameters for training image in SGeMS are channel width, thickness, orientation and net-to-gross ratio (NTG). Channel thickness is ignored since 2D reservoir models are used in this research. The response parameter is oil production rate.

Figure 4.4 shows the result of sensitivity analysis. Channel width and orientation are effective to oil production rate. Therefore, those two parameters are used as uncertainty parameters for the generation of training images.
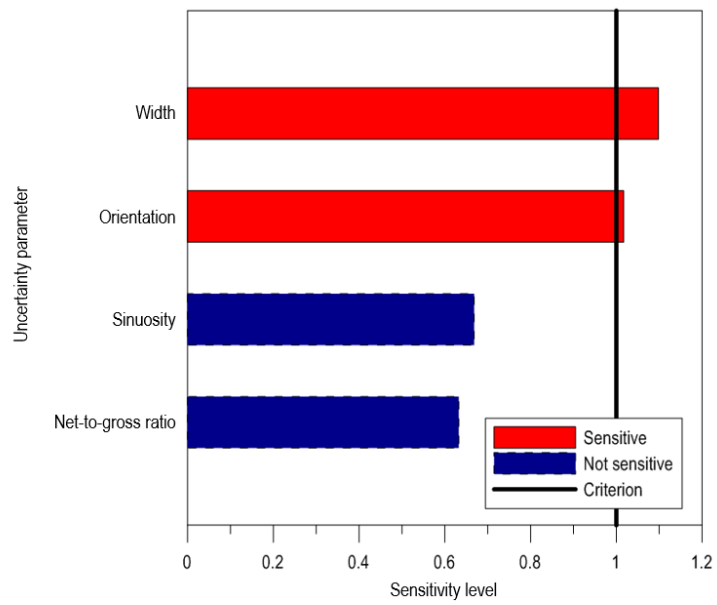
Figure 4.4 Result of sensitivity analysis.

4.2.2. The selection of training images

12 training images varies in channel orientation and width are generated as shown in **Table 4.4**. 360 reservoir models are generated from the training images (30 reservoir models each). Other characteristics of training images are described in **Table 4.5**.

Training images selected are shown in **Figure 4.5**. 4 training images, TI1 (orientation=0°, width=2), TI2 (orientation=0°, width=6), TI3 (orientation=0°, width=10) and TI6 (orientation=45°, width=10), are selected and 3 of them which are TI1, TI2 and TI3 generate facies models that have identical interwell connectivity with the reference field.

Table 4.4 Uncertainty parameters of training images

Training image name	Orientation (°)	Width (unitless)
Reference TI	0	6
TI1	0	2
TI 2	0	6
TI 3	0	10
TI 4	45	2
TI 5	45	6
TI 6	45	10
TI 7	90	2
TI 8	90	6
TI 9	90	10
TI 10	135	2
TI 11	135	6
TI 12	135	10

* Orientation: 0° 45° 90° 135°

Table 4.5 Constant parameters of training images

Parameter	Value
Grid size	250×250
Length (unitless)	10,000
Thickness (unitless)	1
Amplitude (unitless)	5
Net-to-gross ratio (fraction)	0.2

(a) TI2

(b) TI3

(c) TI1

(b) TI6
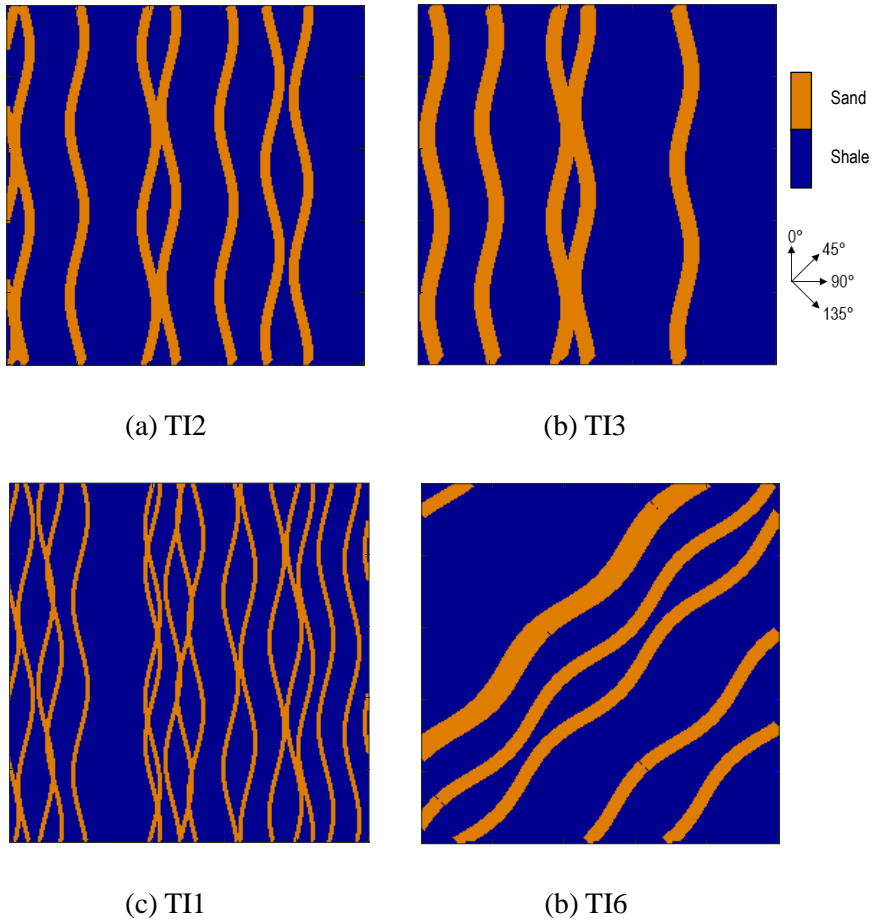
Figure 4.5 Training images selected: (a) TI2 (Orientation is $0°$ and width is 6), (b) TI3 (Orientation is $0°$ and width is 10), (c) TI1 (Orientation is $0°$ and width is 2) and (d) TI6 (Orientation is $45°$ and width is 10).

4.2.3. The reproduction of facies model

Reproduction ratio of training images are shown in **Figure 4.6**. Reproduction of facies model is proceeded using TI1, TI2, TI3 and TI6 that selected in section 4.2.2. Among the reproduced 360 facies models, 65.2% is from TI2, 13.3% is from TI3, 11.3% is from TI6 and 10.2% is from TI1. Training images that generate facies models having identical interwell connectivity with the reference field reproduce 88.7% of total facies models. TI2 which have identical characteristic with the reference field in the perspective of facies distribution reproduces facies models dominantly by 65.2%.

Total 104 facies models are selected from the clustering after simulation with reproduced models.
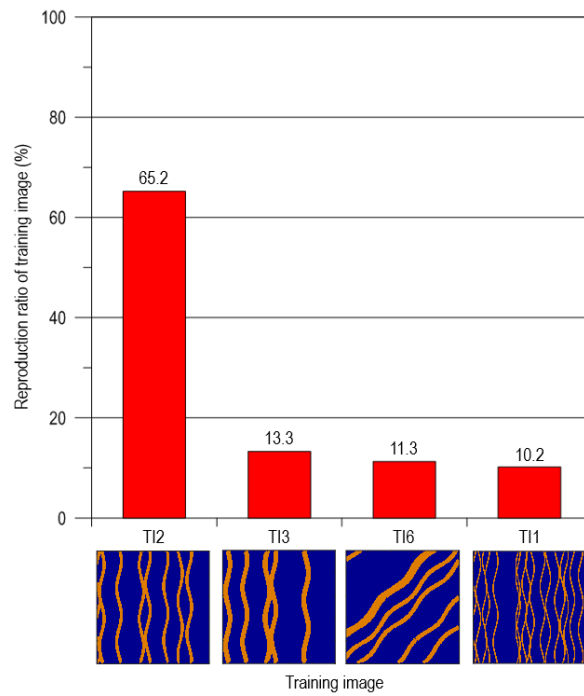
Figure 4.6 Reproduction ratio of training images.

4.3. Evaluation of performance prediction

The history matching and prediction results from the comparison model and proposed model are shown in **Figures 4.7**-**4.10**. In the production estimation of oil, the true value is out of uncertainty range of the comparison model, whereas it is within uncertainty range of the proposed model as shown in **Figures 4.7** and **4.8**. The average relative error between oil production rate of P50 and reference is 90.6% in the comparison model and 19.7% in the proposed model.

The proposed method predicts water breakthrough time more accurately than the comparison model as shown in **Figures 4.9** and **4.10**. Especially, the comparison model make wrong estimation in water production of P2 due to misinterpretation about interwell connectivity between I1 and P2. It expects water breakthrough in P2 on or after the 1000th, whereas there is no water breakthrough in the reference field during the entire prediction period.
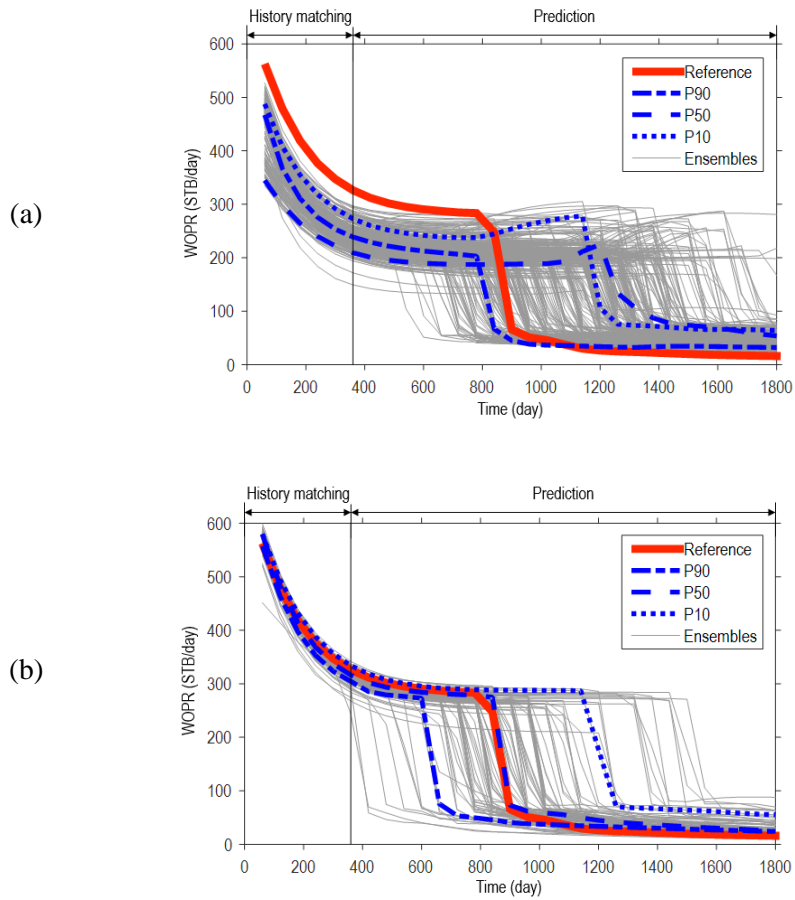
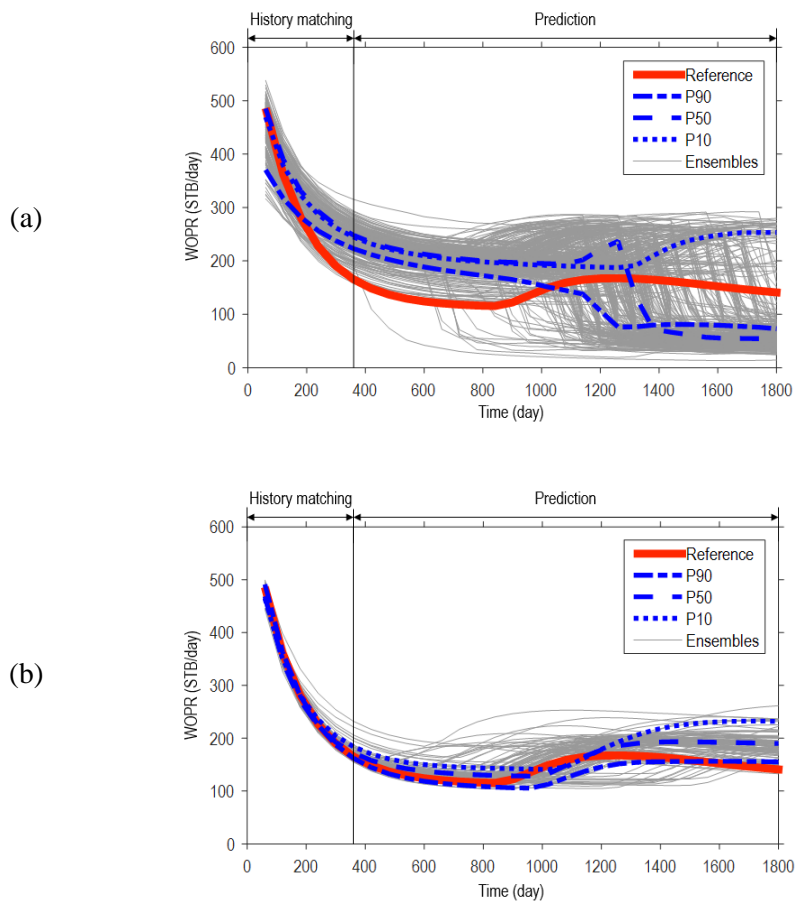**Figure 4.7 Oil production rate of P1: (a) the comparison method and (b) the proposed method.**

Figure 4.8 Oil production rate of P2: (a) the comparison method and (b) the proposed method.
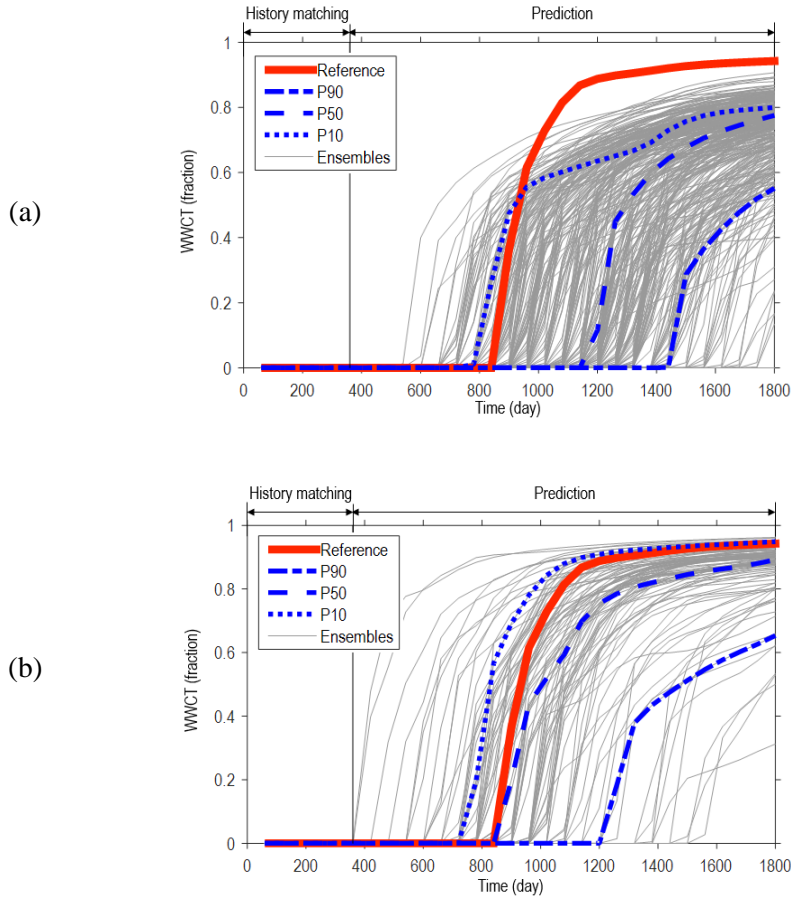
**Figure 4.9 Prediction of water breakthrough time from water cut of P1:
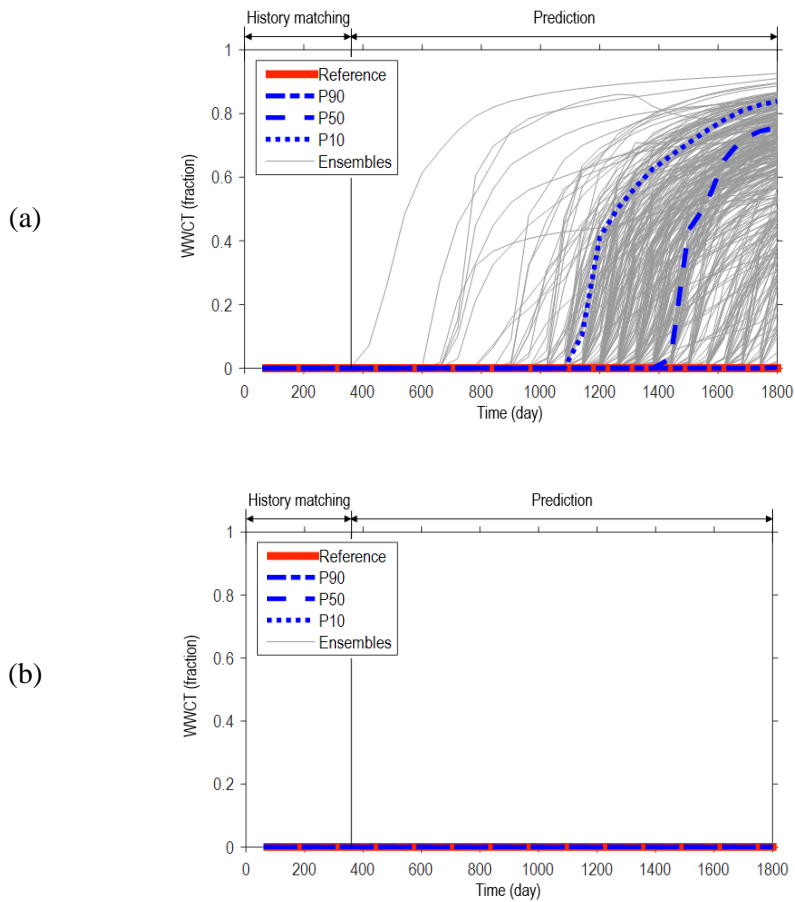(a) the comparison method and (b) the proposed method.**

Figure 4.10 Prediction of water breakthrough time from water cut of P2: (a) the comparison method and (b) the proposed method.

4.4. Effects of multiple training images

Multiple training images are used for generating facies models to consider geological uncertainty. To evaluate the effects of multiple training images, facies models are generated from multiple training images and matched to history using the methods as follows.

- EnKF

- EnKF coupled with clustering

- The proposed method: EnKF coupled with the selection of training image, reproduction of facies model and clustering

The effect of using raw multiple training images and training images passed selection procedure are analyzed in this section.

The results of history matching and prediction are shown in **Figures 4.11**-**4.14**. The original EnKF fails history matching due to the high uncertainty of facies distribution (**Figures 4.11(a)** and **4.12(a)**). Even though the clustering procedure improves accuracy by selecting facies distribution having similar production behavior with the true value, EnKF coupled with clustering fails history matching too (**Figures 4.11(b)** and **4.12(b)**). The proposed model matches history accurately and predicts production performance within allowable error range (**Figures 4.11(c)** and **4.12(c)**). The average relative error between oil production rate of P50 and reference is 36.5% in the result from the

original EnKF, 20.1% in the result from the EnKF coupled with clustering and 19.7% in the result from the proposed model. Also, the proposed method predicts existence of water breakthrough and the time of it accurately as shown in **Figures 4.13** and **4.14**.
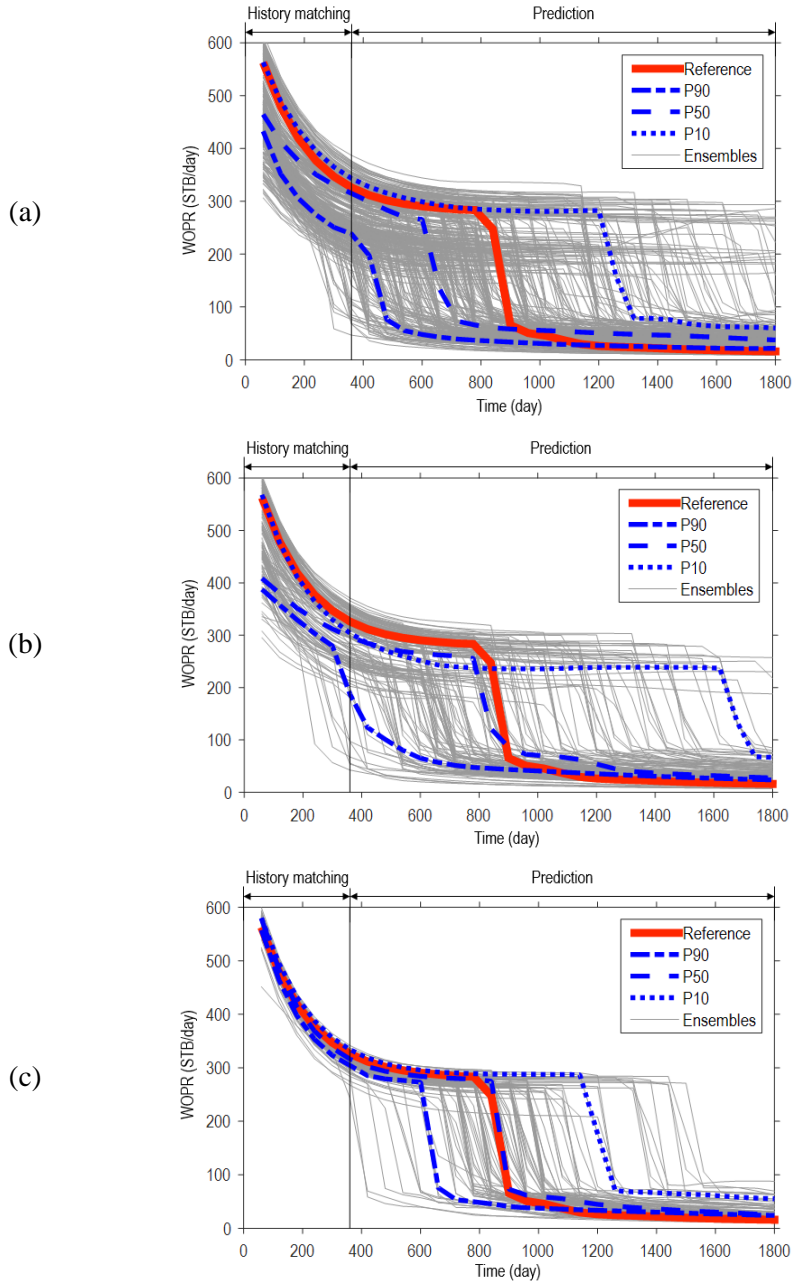
Figure 4.11 Oil production rate of P1: (a) EnKF and (b) EnKF with clustering and (c) the proposed method.
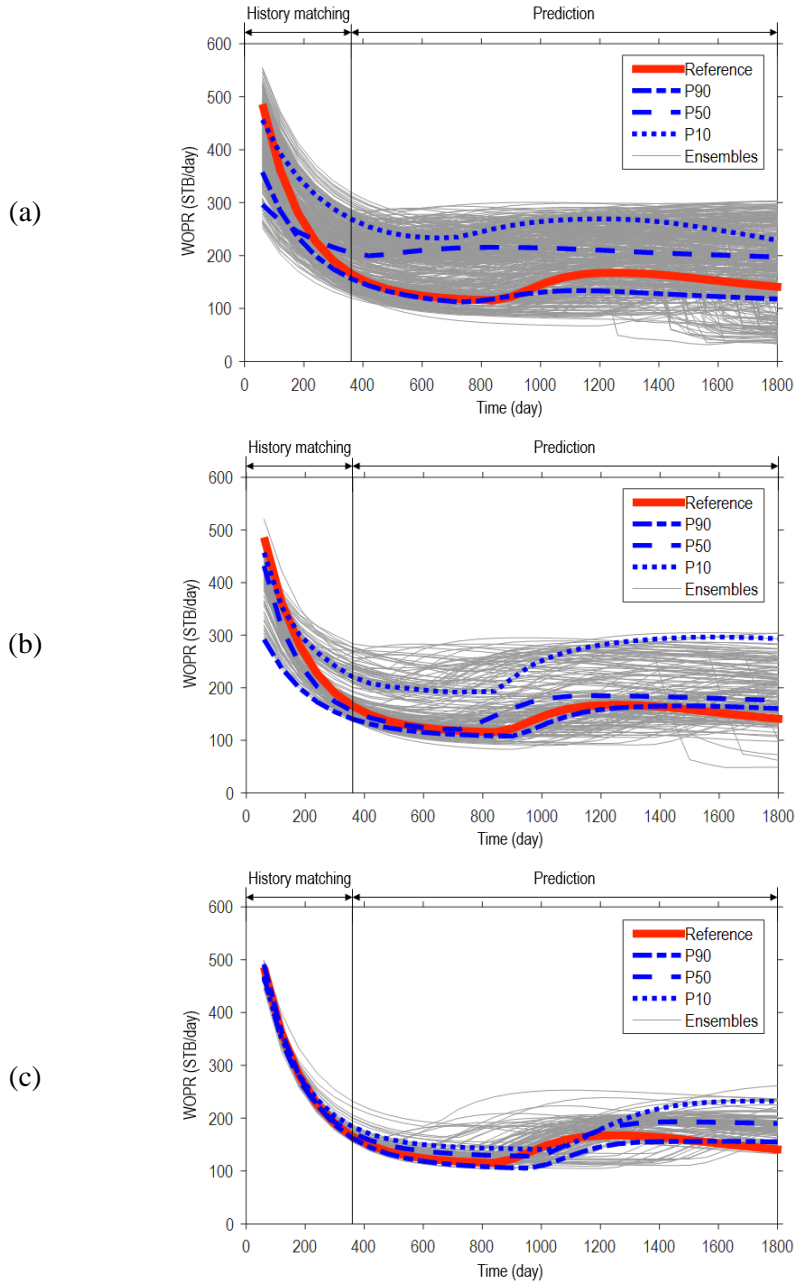
49

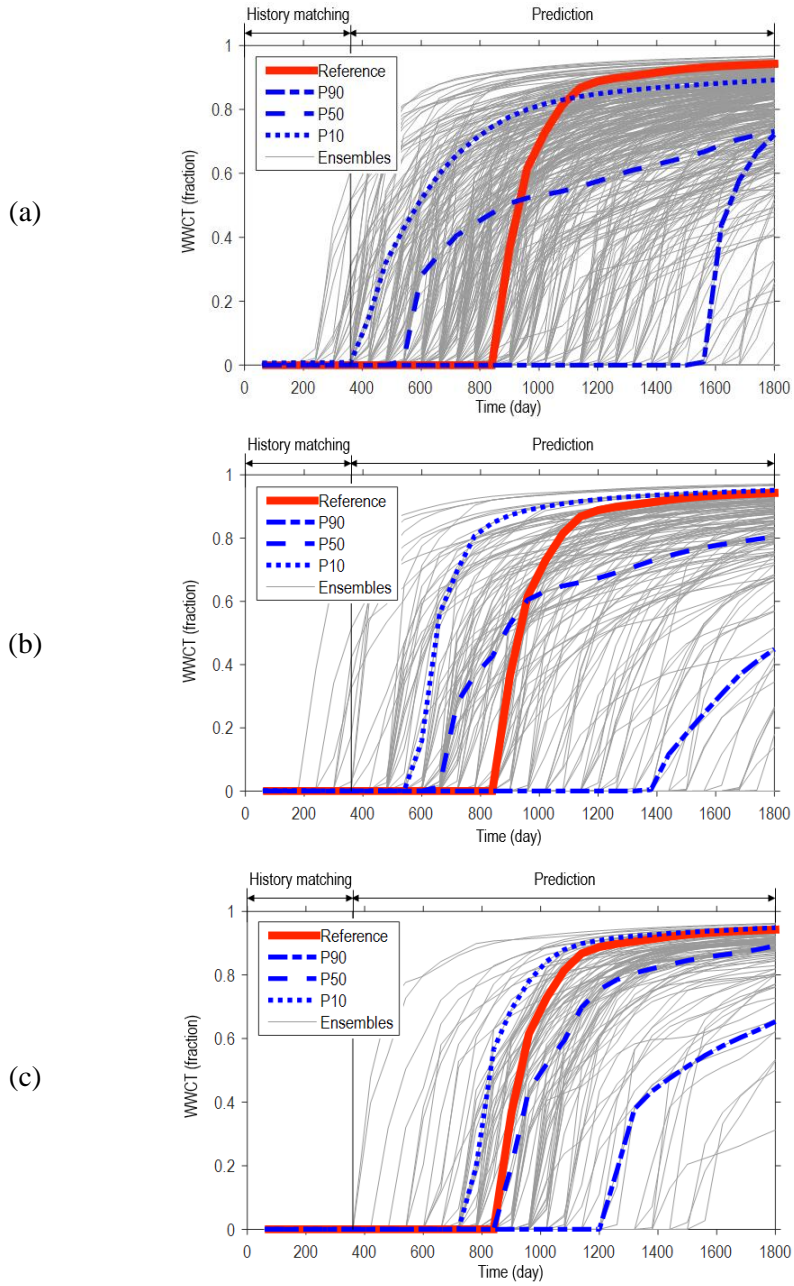**Figure 4.12 Oil production rate of P2: (a) EnKF and (b) EnKF with clustering and (c) the proposed method.**

Figure 4.13 Water cut of P1: (a) EnKF and (b) EnKF with clustering and (c) the proposed method.
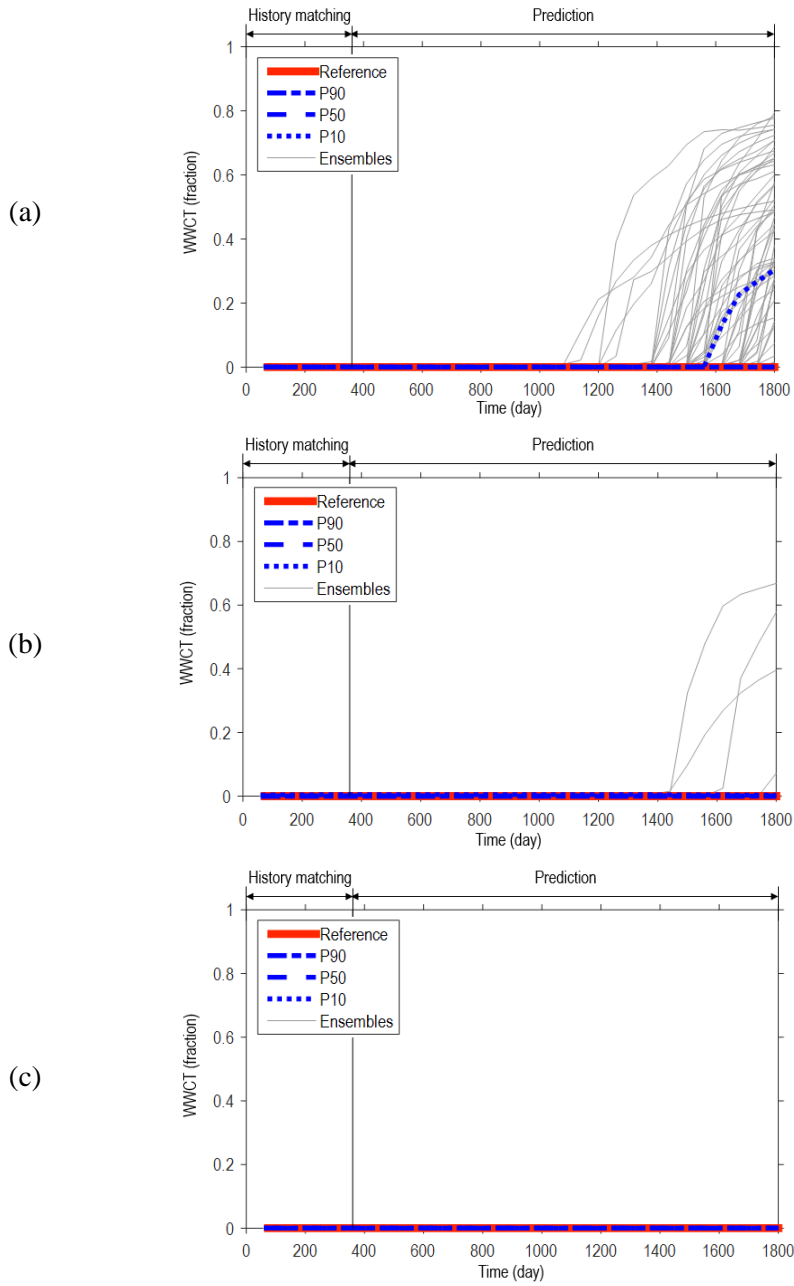
51

Figure 4.14 Water cut of P2: (a) EnKF and (b) EnKF with clustering and (c) the proposed method.

4.5. Robustness test

The situation adding a new Injection well is assumed. Prediction is proceeded assuming a new injection well, I2, is added at the location of (1,900 ft, 1,750 ft). Facies distribution and well location in the results from each method is described in **Figure 4.15**. I2 starts water injection at 360th day. The production changes due to the additional water injection are shown in **Figures 4.16**-**4.19**. The average relative error between oil production rate of P50 and reference is 51.1% in the result of the comparison model, 21.0% in the result of the proposed model. Also, the proposed method predicts the water breakthrough time and oil-water ratio more accurately than the comparison model as shown in **Figures 4.18** and **4.19**. The proposed model is able to predict future production with the change in well composition accurately based on reliable prediction of facies distribution.
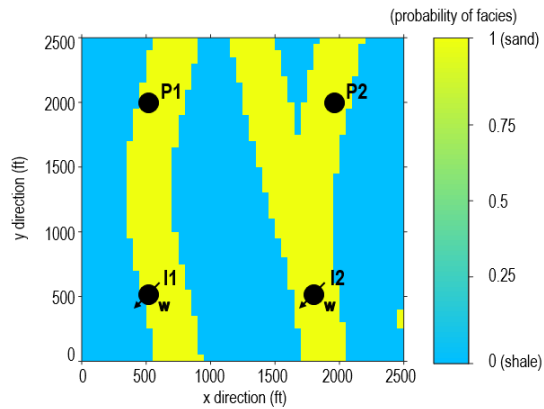
(a) Facies distribution of the reference field
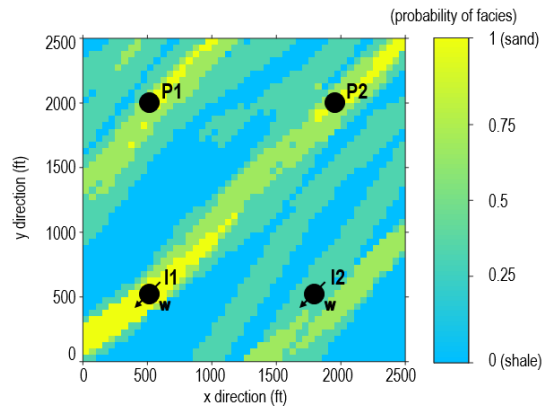
(b) Mean of facies distributions of the comparison model
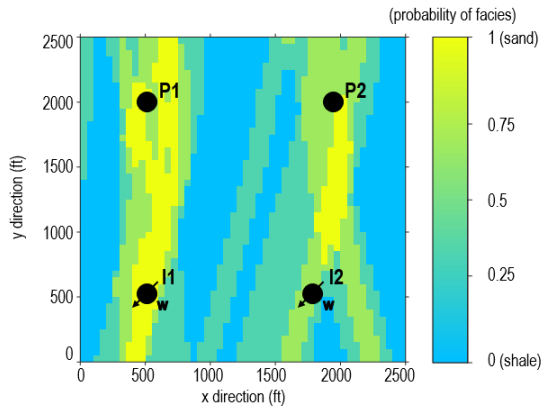
(c) Mean of facies distributions of the proposed model

Figure 4.15 Facies distribution and the location of newly added well, I2.

Figure 4.16 Oil production rate of P1: (a) the comparison method and (b) the proposed method. Red line describes the true value in case the new well, I2, injects water and pink line describes the true value in case no well added. Blue lines are P10, 50, 90.
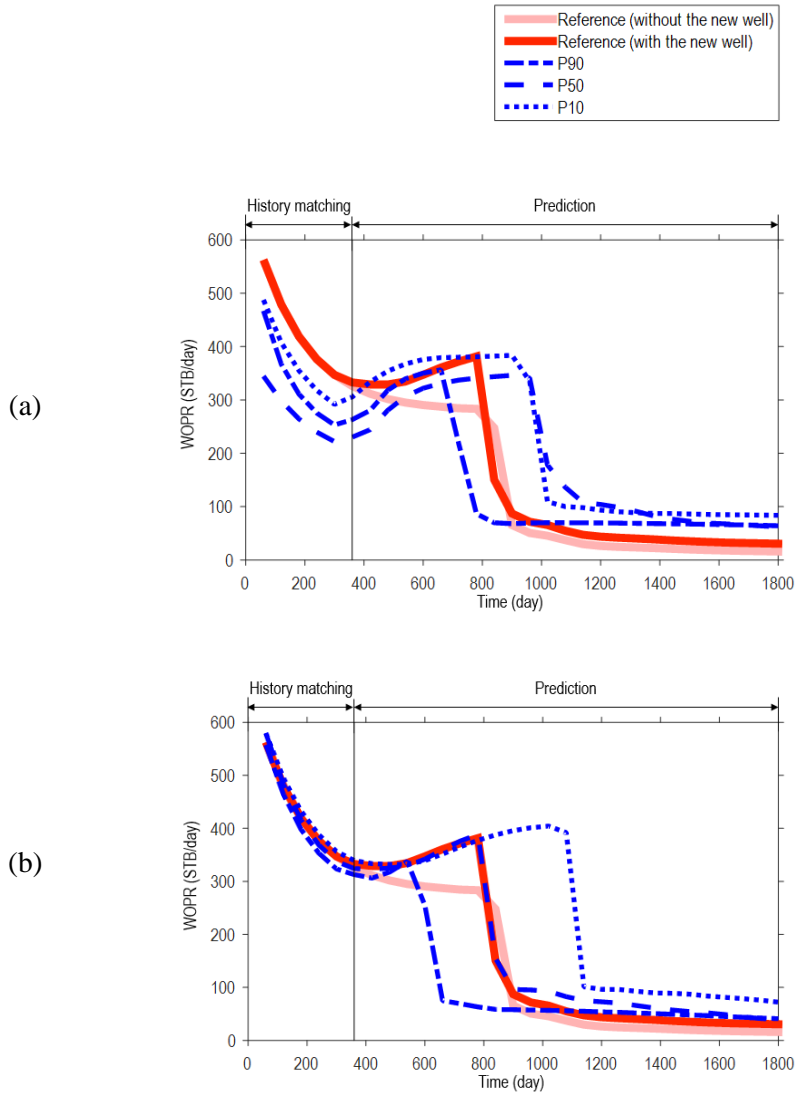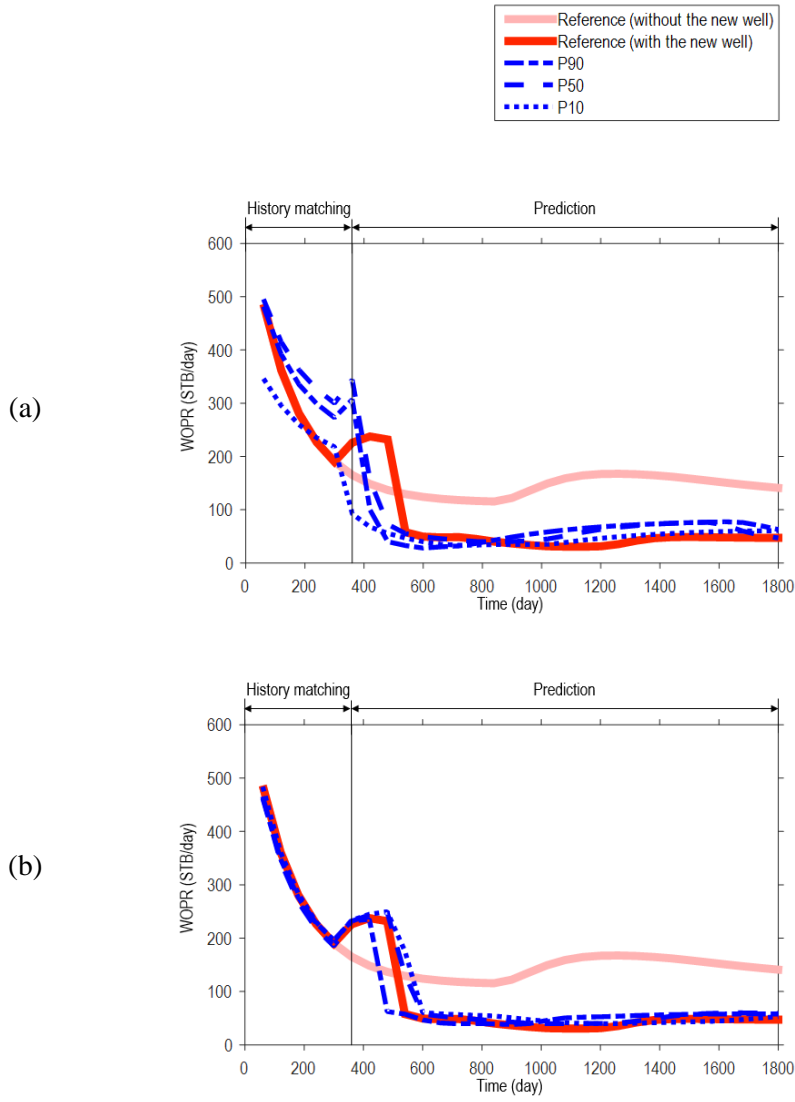
Figure 4.17 Oil production rate of P2: (a) the comparison method and (b) the proposed method. Red line describes the true value in case the new well, I2, injects water and pink line describes the true value in case no well added. Blue lines are P10, 50, 90.

Figure 4.18 Water cut of P1: (a) the comparison method and (b) the proposed method. Red line describes the true value in case the new well, I2, injects water and pink line describes the true value in case no well added. Blue lines are P10, 50, 90.

Figure 4.19 Water cut of P2: (a) the comparison method and (b) the proposed method. Red line describes the true value in case the new well, I2, injects water and pink line describes the true value in case no well added. Blue lines are P10, 50, 90.
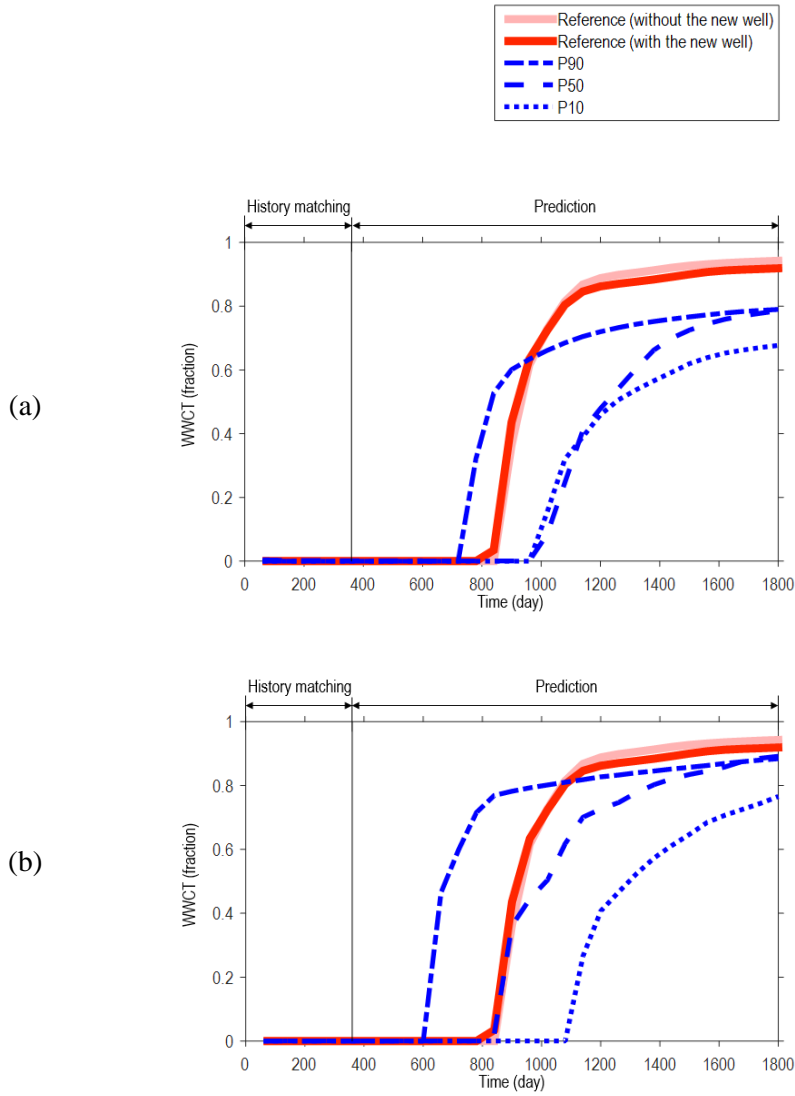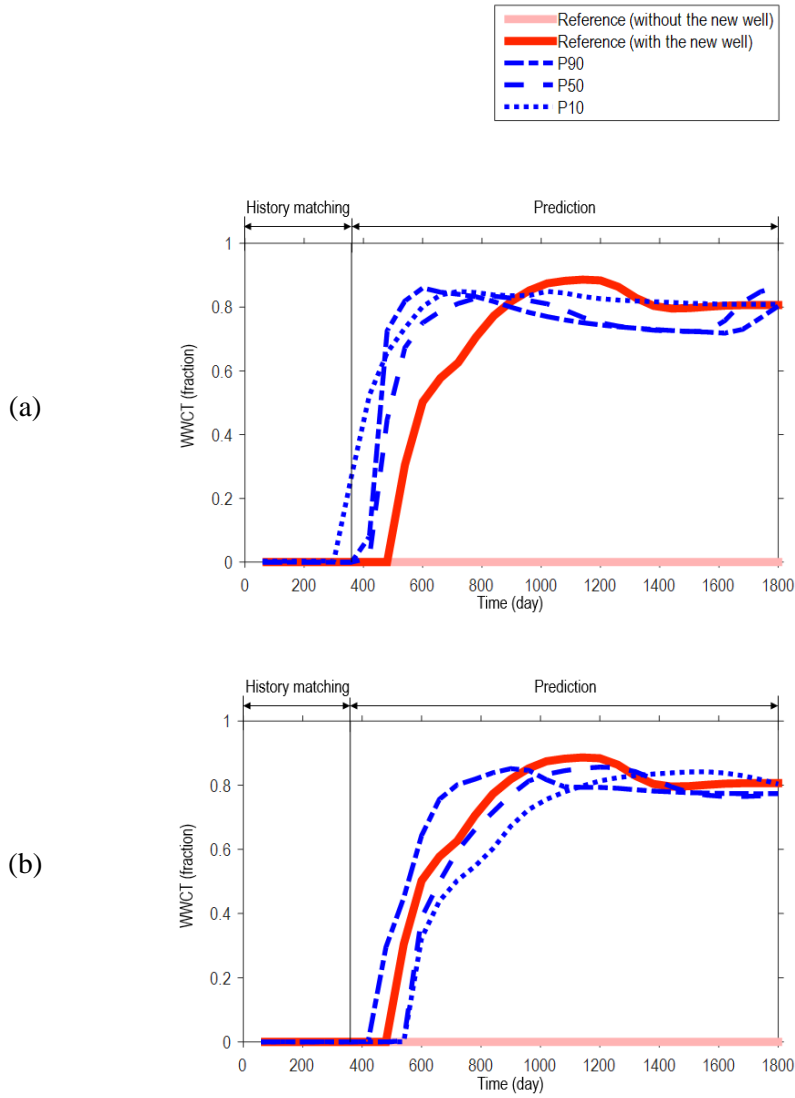
4.6. Discussion

The developed model improves prediction performance of production behavior based on reliable facies model obtained from the preprocess integrating dynamic and static data. However, the proposed model finishes prediction of facies distribution at the preprocessing step—step1. Selection of training image and step2. Reproduction of facies model. In history matching step with Ensemble Kalman Filter, it modifies permeability distribution while faices distribution is fixed. To improve the performance of the proposed model, it is recommended to reproduce facies itself by applying a tool that can suggest criteria such as level set method. Additionally, this approach will be efficient to maintain bimodal distribution, which is representative characteristic of channeled reservoir.

5. Conclusions

This paper develops a new history matching method that allows reliable prediction of facies distribution and production performance by integrating dynamic and static data. The conclusions are as follows.

1. This paper proposes the history matching method that can predict both facies and permeability distribution reliably by Ensemble Kalman Filter coupled with distance-based method. The closest training images to observed history are selected using distance-based method to integrate the static data. Facies and permeability distributions are estimated and future production is predicted by reproducing the facies model from the selected training images and history matching with Ensemble Kalman Filter.

2. The proposed method predicts interwell connectivity with 88.7% accuracy. The prediction error for the oil production rate using the proposed method is 70.9% lower than that using the conventional method.

3. Multiple training images allows securing diversity but it is hard to characterize the facies model due to its high uncertainty. The selection procedure reduces the prediction error for production performance by 16.6% on average compared to Ensemble Kalman Filter without a selection procedure. The proposed method predicts the water breakthrough time more accurately than the other methods by around 200 days.

4. The proposed method is able to predict the facies distribution reliably using dynamic data without a water breakthrough time. The method accurately predicts the production change originated from adding a new injection well based on reliable prediction of the facies distribution.

This paper can contribute to reliable prediction of production performance and reasonable decision making based on the ability that predicts facies distribution stably and accurately.

References

Anterion, F., Eymard, R., and Karcher, B. 1989. Use of Parameter Gradients for Reservoir History Matching. Paper SPE 1844 presented at the SPE Symposium on Reservoir Simulation, Houston, Texas, 6-8 February. http://dx.doi.org/10.2118/18433-MS

Caers, J. 2011. *Modeling Uncertainty in the Earth Sciences*. Chichester, UK: John Wiley & Sons Ltd. http://dx.doi.org/10.1002/9781119995920

Evensen, G. 1994. Sequential Data Assimilation with a Nonlinear Quasi-geostrophic Model using Monte Carlo Methods to Forecast Error Statistics. *Journal of Geophysical Research* **99** (C5): 10143-10162. http://dx.doi.org/10.1029/94JC00572

Fenwick, D., Scheidt, C., and Caers, J. 2014. Quantifying Asymmetric Parameter Interactions in Sensitivity Analysis: Application to Reservoir Modeling. *Mathematical Geosciences* **46**: 493-511. http://dx.doi.org/10.1007/s11004-014-9530-5

Gu, Y. and Oliver, D.S. 2005. History Matching of the PUNQ-S3 Reservoir Model using the Ensemble Kalman Filter. *SPE Journal* **10** (2): 217-224. SPE-89942-PA. http://dx.doi.org/10.2118/89942-PA

Guardiano, F. and Srivastave, R.M. 1993. *Multivariate Geostatistics: Beyond Bivariate Moments.* Soares, A. ed., *Geostatistics-Troia*, Kluwer, Dordrecht, Holland.

Lee, K. 2014. *Channelized Reservoir Characterization using Ensemble Smoother with a Distance-based Method.* PhD dissertation, Seoul National University, Seoul (April 2014)

Lorentzen, R.J., Flornes, K.M., and Næ vdal, G. 2012. History Matching Channelized Reservoirs using the Ensemble Kalman Filter. *SPE J*. **17** (1): 137-151. SPE-143188-PA.   http://dx.doi.org/10.2118/143188-PA

Næ vdal, G. and Vefring, E.H. 2002. Near-well Reservoir Monitoring through Ensemble Kalman Filter. Paper SPE 75235 presented at the SPE/DOE Improved Oil Recovery Symposium, Tulsa, Oklahoma, 13-17 April. http://dx.doi.org/10.2118/75235-MS

Park, K. 2008. Ensemble Kalman Filtering in Distance Kernal Space. 21st SCRF Annual Meeting Report.

Roggero, F., Hu, L.Y., and Helios Reservoir Group. 1998. Gradual Deformation of Continuous Geostatistical Models for History Matching. Paper SPE 49004 presented at the SPE Annual Technical Conference and Exhibition, New Orleans, Louisiana, 27-30 September. http://dx.doi.org/10.2118/49004-MS

Sarma, P. and Chen, W. H. 2009. Generalization of the Ensemble Kalman Filter using Kernels for Nongaussian Random Fields. Paper SPE 119177 presented at the SPE Reservoir Simulation Symposium, Woodlands, Texas, 2-4 February. http://dx.doi.org/10.2118/119177-MS

Scheidt, C. and Caers, J. 2009. Representing Spatial Uncertainty using Distances and Kernels. *Mathematical Geosciences* **41** (4): 397-419. http://dx.doi.org/10.1007/s11004-008-9186-0

Schulze-Riegert, R., Axmann, J.K., Haase, O., Rian, D.T., and You, Y.L. 2002. Evolutionary Algorithms Applied to History Matching of Complex Reservoirs. Paper 77301 presented at the SPE Reservoir Simulation Symposium, Houston, Texas, 11-14 February. SPE-77301-PA. http://dx.doi.org/10.2118/77301-PA

Soleng, H. 1999. Oil Reservoir Forecasting with Uncertainty Estimation using Genetic Algorithms. *Proceedings of the Congress on Evolutionary Computing*, IEEE, Washington, 6-9 July. http://dx.doi.org/10.1109/CEC.1999.782574

Suzuki, S. and Caers, J. 2006. History Matching with an Uncertainty Geological Scenario. Presented at the SPE Annual Technical Conference and Exhibition, San Antonio, Texas, 24-27 September. http://dx.doi.org/10.2118/102154-MS

Strebelle, S. 2002. Conditional Simulation of Complex Geological Structures using Multiple-point Statistics. *Mathematical Geology* **34** (1): 1-21. http://dx.doi.org/10.1023/A:1014009426274

Appendix A. Determination of the optimum number of training images

The purpose of the selection of reservoir models using distance-based method is increasing accuracy of history matching by characterizing channels using reservoir models showing similar production behavior with observed data. Selecting few reservoir models has risk that only improper training images are to be selected and selecting too many reservoir models results in high uncertainty. Accuracy of history matching decreases in both cases. Therefore, it is important to select the proper number of reservoir models that makes proper training images selected most dominantly.

Figure A.1 shows the average probability of improper training images to be selected depending on the selecting number of reservoir models. For the generalization of selecting number, the selection procedure was conducted several times using diverse reference fields having different interwell connectivity. The proper training image is defined as the training image that has identical value with the training image of each reference field in the perspective of channel width and orientation. The other training images are regarded as improper ones.

The performance of the selection is the most accurate when the 5 nearest models are selected on average. Therefore, 5 reservoir models are selected at every response parameter.
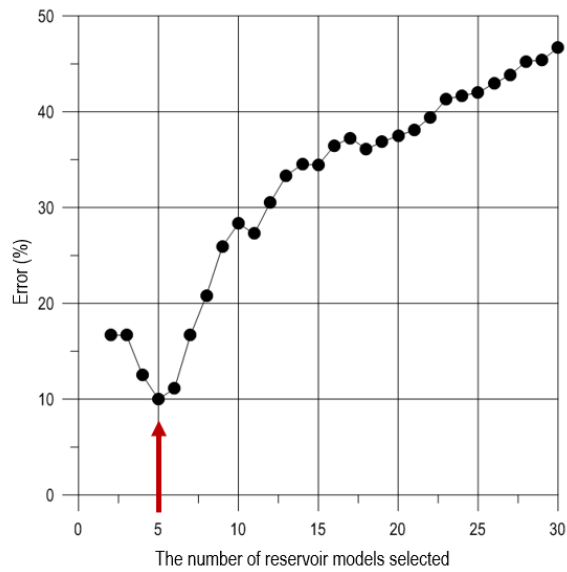
Figure A.1 Error variance depending on the number of selected reservoir models.

요약(국문초록)

이 연구는 동적 및 정적 자료의 통합을 통해 불균질 저류층의 유체 생산추이 예측성능을 향상시키고, 유정 간 유체거동 연결성을 규명할 수 있는 히스토리매칭 모델을 개발하였다. 기존 히스토리매칭은 주로 동적 자료의 매칭에 집중하였기 때문에, 정적 물성과 암종 분포의 예측은 불가능하였고 장기적인 생산추이 예측의 신뢰도가 낮았다. 이 연구에서 개발한 히스토리매칭 기법은 정적 자료의 불확실성을 포함한 다수의 트레이닝 이미지를 생성한 후 거리기반방법을 이용한 트레이닝 이미지 선택을 통해 암종 분포를 예측하였다. 예측한 암종 분포를 따르는 저류층 모델을 다점지구통계기법을 이용하여 재생산하고 히스토리매칭하였다. 트레이닝 이미지 선택 결과 유정 간 연결성을 88.7%의 높은 확률로 예측하였다. 저류층 물성 교정만 가능했던 기존의 히스토리매칭 기법과는 달리 암종모델 전처리 과정을 거친 제안 기법은 저류층 물성과 암종 분포의 교정이 모두 가능하였다. 기존 방법에 비해 유체 생산추이의 오차가 70.9% 감소되어 향상된 예측성능을 보였다. 물돌파 정보가 없는 경우에도 암종모델의 높은 신뢰도를 확보함으로써 실제 생산추이에 가깝게 예측하였다. 이 연구결과는 동적 및 정적자료의 통합을 통해 신뢰도 높은 암종모델을 구성할 수 있어, 생산추이 예측의 안정성을 제고하고 합리적인 생산설계를 가능하게 한다.